

## Synthesis of Tetrathiafulvalene-Functionalized Organic-Metal Hybrid Polymer

Taichi Ikeda, Masayashi Higuchi\* and Dirk G. Kurth

Functional Modules Group, Organic Nanomaterials Center, National Institute for Materials Science  
 Fax: 81-29-860-4721, e-mail: IKEDA.Taichi@nims.go.jp

\* Functional Modules Group, Organic Nanomaterials Center, National Institute for Materials Science  
 Fax: 81-29-860-4721, e-mail: HIGUCHI.Masayoshi@nims.go.jp

The electrochemically-active ligand has synthesized, in which the tetrathiafulvalene module is introduced at the 6-position of 1,4-di(2,2':6',2''-terpyridin-4'-yl)benzene (TTF-bTP). The synthesis was confirmed by MALDI-TOF MS and  $^1\text{H}$  NMR. The organic-metal hybrid polymer consisting of TTF-bTP and Fe(II) was prepared. The formation of the hybrid polymer was monitored by UV-Vis spectrum titration and confirmed the polymeric objects by atomic force microscopy (AFM).

Key words: Organic-metal hybrid polymer, Coordination chemistry, Tetrathiafulvalene

### 1. INTRODUCTION

The coordination polymers consisting of the transition metals and the bi-functional terpyridine derivatives, e.g. 1,4-di(2,2':6',2''-terpyridin-4'-yl)benzene (bTP), are of great interest in the field of the material science.<sup>1-6</sup> We also have synthesized organic-metallic hybrid polymers consisting of the bTP and transition metals such as  $\text{Fe}^{2+}$ ,  $\text{Co}^{2+}$ ,  $\text{Ru}^{2+}$  (Fig. 1a).<sup>7</sup> We have called those hybrid materials as the metallo-supramolecular coordination polyelectrolyte (MEPE),<sup>8</sup> and studied as an electrochemically-active polymer material. The materials with the transition metals of  $\text{Fe}^{2+}$  and  $\text{Ru}^{2+}$  have characteristic colors based on the metal-to-ligand charge-transfer (MLCT) absorption band.<sup>1,7</sup> The MLCT band disappears when the transition metal is oxidized, i.e.  $\text{Fe}^{2+} \rightarrow \text{Fe}^{3+}$ . Thus these hybrid polymers are the promising candidates for the electrochromic devices like the electric paper displays.<sup>9</sup>

introduced at the 6-position of 1,4-di(2,2':6',2''-terpyridin-4'-yl)benzene. Furthermore, the MEPE was prepared from the mixture of the TTF-bTP and  $\text{Fe}^{2+}$  (Fig. 1b). The formation of the MEPE was confirmed by UV-Vis titration and atomic force microscopy (AFM) experiments.

### 2. EXPERIMENT

#### 2.1. General

(Hydroxymethyl)tetrathiafulvalene (TTF-OH)<sup>10</sup> and 1-(6-bromo-2,2':6',2''-terpyridin-4'-yl)-4-(2,2':6',2''-terpyridin-4'-yl)benzene (Br-bTP)<sup>11</sup> were synthesized according to the literatures. The UV-Vis titration measurement was conducted as follows. The solutions of TTF-bTP ( $\text{CHCl}_3$ ,  $1.0 \times 10^{-5}$  M) and  $\text{Fe}(\text{BF}_4)_2 \cdot 6\text{H}_2\text{O}$  ( $\text{MeOH}$ ,  $5.0 \times 10^{-4}$  M) were prepared. The solution of the  $\text{Fe}(\text{BF}_4)_2$  was added stepwise to the TTF-bTP solution. The UV-Vis spectrum was recorded at each step and the effect of the dilution was calibrated based on the Lambert-Beer's law. For AFM measurement, the solution of  $\text{Fe}(\text{TTF-bTP})(\text{BF}_4)_2$  ( $\text{CHCl}_3/\text{MeOH}$ , 1  $\mu\text{M}$ ) was prepared. The sample was prepared on the freshly-cleaved high oriented pyrolytic graphite (HOPG) surface by spin coating. The sample substrate was rinsed gently using distilled water before AFM observation. The observation was conducted on the DFM mode under air at room temperature (S-image controlled with SPI 4000 probe station, SII NanoTechnology Inc.).

#### 2.2 Synthesis of TTF-bTP

TTF-OH (250 mg, 1.1 mmol) was dissolved in 50 mL of dry THF, and NaH (100mg) was added to the solution. The mixture was heated under reflux for 4h. Br-bTP (200mg,  $3.2 \times 10^{-4}$  mol) was added to the solution and heated under reflux for more 16h. After cooling to 0 °C, the NaH was quenched by the mixture ( $\text{Me}_2\text{CO} / \text{H}_2\text{O} = 9/1$ ). The solution was dried with  $\text{MgSO}_4$ , filtrated and evaporated. The product was subjected to column chromatography ( $\text{Al}_2\text{O}_3$ ,  $\text{CHCl}_3/\text{hexane} = 3/2$  and  $\text{CHCl}_3/\text{acetone} = 4/1$ ). The crude product was purified

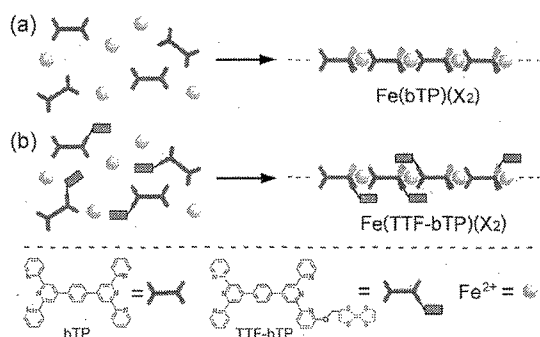


Fig. 1 Schematic representation for the preparation of organic-metal hybrid polymers. (a)  $\text{Fe}(\text{bTP})(\text{X}_2)$ , (b)  $\text{Fe}(\text{TTF-bTP})(\text{X}_2)$ . X: counter ion.

In this study, we synthesized novel electrochemically-active ligand (TTF-bTP), in which the tetrathiafulvalene (TTF) module is

by the recycling preparative HPLC (Column: JAIGEL-1H and JAIGEL-2H, Controller: LC-9104, Japan Analytical Industry Co. Ltd.). The product was obtained as yellow solid. Yield: 100 mg (40%).  $^1\text{H NMR}$  (300 MHz,  $\text{DMF-}d_7$ ):  $\delta$  = 5.54 (s,  $\text{CH}_2$ ), 6.73 (m,  $\beta$ ), 7.07 (overlapping,  $\alpha$ , 5), 7.58 (dd,  $J$  = 4.95, 6.60 Hz, 5''), 8.02 – 8.15 (m, 4, 4''), 8.24 – 8.36 (m, Ph), 8.47 (d, I = 7.32 Hz, 3), 8.80 – 8.86 (overlapping, 3'', 6''), 8.95 (s, 5'), 9.01 ppm (s, 3'); MS (MALDI-TOF):  $m/z$  = 772.09  $[\text{M}]^+$ .

### 3. RESULTS AND DISCUSSIONS

#### 3.1 Synthesis of TTF-bTP

The electrochemically-active ligand TTF-bTP was synthesized by the coupling between Br-bTP and sodium methoxide TTF. Fig. 2 shows the  $^1\text{H NMR}$  spectrum of the TTF-bTP. We can confirm all of the protons belonging to TTF and bTP moieties. The successful purification was confirmed by MALDI-TOF MS as well. The spectrum shows only the peaks corresponding to the molecular weight of TTF-bTP.

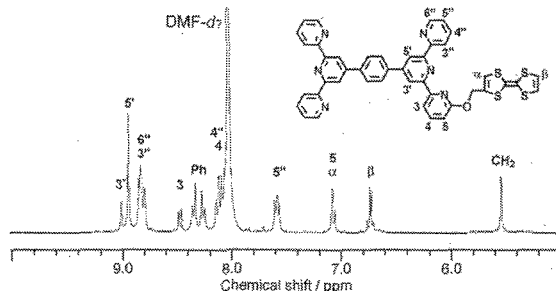


Fig. 2  $^1\text{H NMR}$  spectrum of TTF-bTP (RT, 300MHz,  $\text{DMF-}d_7$ )

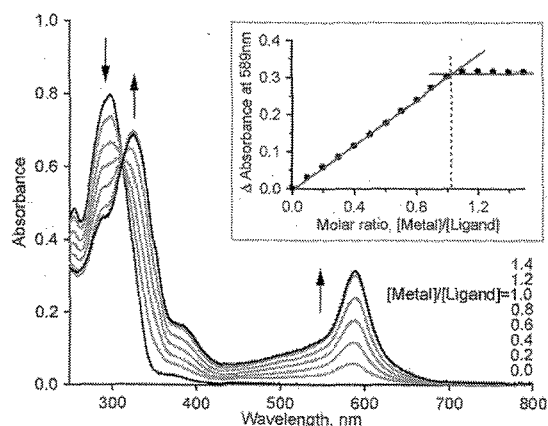


Fig. 3 UV-Vis spectrum change in the titration of  $\text{Fe}(\text{BF}_4)_2$  to the TTF-bTP solution. (inset) The change in the absorbance at 589nm.

#### 3.2 UV-Vis titration for the preparation of MEPE

The formation of the MEPE consisting of TTF-bTP and  $\text{Fe}^{2+}$  [Fig. 1 (b)] was confirmed by UV-Vis titration measurement. Fig. 3 shows the results of UV-Vis titration experiment. Before the addition of  $\text{Fe}(\text{BF}_4)_2$ , the peak corresponding to the ligand-centered absorption was detected ( $\lambda_{\text{max}} = 297 \text{ nm}$ ). The solution was colorless because of the no absorption peaks in the visible region. When the  $\text{Fe}(\text{BF}_4)_2$  solution was added to the TTF-bTP solution, the color of the solution turned

blue purple. This color arises from the MLCT band ( $\lambda_{\text{max}} = 589 \text{ nm}$ ). In the same time, we detected the red shift of the ligand-centered absorption bands ( $\lambda_{\text{max}} = 297 \text{ nm} \rightarrow 325 \text{ nm}$ ). These results are well-consistent with those previously reported on the formation of the terpyridine- $\text{Fe}^{2+}$  complexes.<sup>12</sup>

In order to determine the stoichiometry for the complex formation, the relationship between the absorbance at 589 nm and the molar ratio ( $[\text{Metal}]/[\text{Ligand}]$ ) is plotted (Fig. 3 inset). The intensity of the MLCT band increased in proportional to the molar ratio, then reached the saturation around one. From this plot, we confirmed that the TTF-bTP and  $\text{Fe}^{2+}$  forms a 1:1 complex. This result is in good agreement with what we expect from the structure depicted in Fig. 1.

#### 3.3 AFM measurement

The polymeric structure of the MEPE was confirmed by AFM. The sample was spin-coated on a freshly-cleaved HOPG surface. Fig. 4 shows the representative one of the AFM images. The long strands (b in Fig. 4) over the graphite steps (a in Fig. 4) are detectable. The length of some strands exceeds one micro meter. In the successive AFM measurement, we observed the diffusion of the strands along to the scanning direction. This is due to a small adhesive force of the MEPE on the graphite surface. The molecule with the flat structure<sup>13</sup> or the long alkyl chains<sup>14</sup> can adsorb strongly on the surface. However, the MEPE  $\text{Fe}(\text{TTF-bTP})(\text{BF}_4)_2$  has neither of these properties.

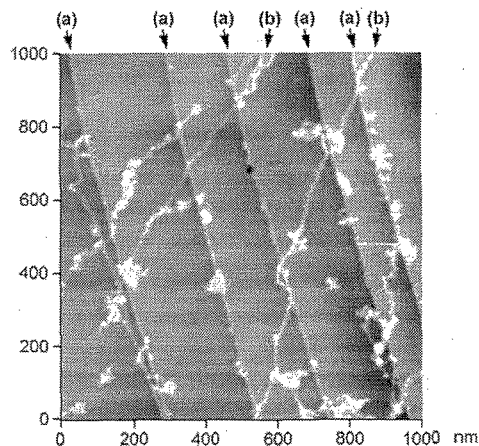


Fig. 4 AFM image of the MEPE  $[\text{Fe}(\text{TTF-bTP})(\text{BF}_4)_2]$  on the graphite surface. The arrow (a) and (b) indicates the graphite steps and the sample strands, respectively.

In order to confirm whether the observed strands are MEPE  $\text{Fe}(\text{TTF-bTP})(\text{BF}_4)_2$  or not, we compared the dimensions obtained from the AFM section profile and the calculated model structure. We confirmed the thickness of the strand to be 0.9 nm from the AFM section profile [Fig. 5 (a)]. We selected a model compound consisting of  $\text{Fe}^{2+}$  ion and two ligands 6-TTFmethoxy-4'-phenyl-2,2':6',2''-terpyridine [ $\text{Fe}(\text{TTF-mTP})_2$ ] to calculate the optimized structure of the MEPE  $\text{Fe}(\text{TTF-bTP})(\text{BF}_4)_2$ . Fig. 5 (b) shows the optimized structure of  $\text{Fe}(\text{TTF-mTP})_2$  by MM3 calculation. The calculated thickness of the model compounds are also 0.9 nm. The same dimension between the observed and

calculated structure strongly supports the fact that the observed strands in the AFM image should be the single strand of the MEPE  $\text{Fe}(\text{TTF-bTP})(\text{BF}_4)_2$ .

As can be seen in Fig. 5 (b), the structure of the ligand is distorted by the steric hindrance of the TTF moiety. It is expected that this distortion suppresses the association constant between the TTF-side terpyridine units and  $\text{Fe}^{2+}$  ion, and results in the shorter chain length. However, we could detect long strands in the AFM image (Fig. 4). This result suggests that the steric effect of TTF moiety on the complex formation is not significant. However, it is notable that the degree of polymerization depends not only on the association constant between the transition metal and the ligand but also on the concentration of the solution.<sup>15</sup> Thus, the supramolecular polymeric structure can develop in the evaporation process of the solvent even in the case of the relatively smaller association constants. In the titration experiment, we confirmed a linear increase in the MLCT band up to the saturation (Fig. 3 inset). This result suggests that the association constant between the TTF-side terpyridine units and the  $\text{Fe}^{2+}$  ion should be comparable to that for the non-substituted terpyridine units.

The globular objects scattered on the surface are considered to be the impurities including in the chemicals [ $\text{Fe}(\text{BF}_4)_2 \cdot 6\text{H}_2\text{O}$  and solvents] or the stacked MEPE strands. Most of these are along the MEPE strands or the graphite steps. As mentioned above, the adhesive force of the MEPE to the graphite surface is small. Thus, the MEPE strands easily diffuse on the surface and stacked at the protrusion part on the surface in the sample preparation process.

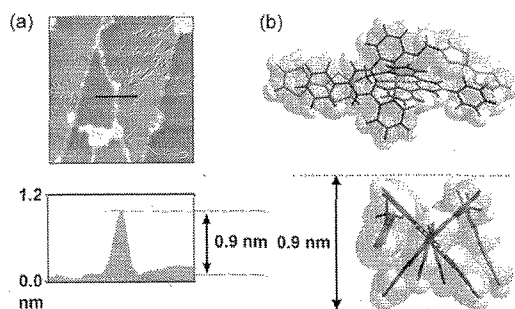


Fig. 5 (a) Section profile of the AFM image. (b) Partial molecular structure of the complex  $\text{Fe}(\text{TTF-mTP})_2$  optimized by MM3 calculation.

#### 4. CONCLUSION

In this study, we synthesized the novel ligand with electrochemically-active TTF moiety (TTF-bTP). The synthesis of the ligand was confirmed by  $^1\text{H}$  NMR and MALDI-TOF MS. The formation of MEPE  $\text{Fe}(\text{TTF-bTP})(\text{BF}_4)_2$  was confirmed by AFM. AFM image revealed the fibrous supramolecular structure of MEPE. The electrochemically-active supramolecular fibers are attractive materials for 1-dimensional conducting wires.<sup>16</sup> The regioregularity of the ligand in the MEPE, *i.e.* head-to-tail or head-to-head, and the electrochemistry of the MEPE  $\text{Fe}(\text{TTF-bTP})(\text{BF}_4)_2$  are now under investigation.

#### ACKNOWLEDGEMENT

This work was financially supported by "Grant-in-Aid for Young Scientists B," 19710102.

#### REFERENCES

- [1] S. Bernhard, J. I. Goldsmith, K. Takada, H. Abruña, *Inorg. Chem.*, **42**, 4389-93 (2003); J. A. Barron, S. Glazier, S. Bernhard, K. Takada, P. L. Houston, H. D. Abruña, *Inorg. Chem.*, **42**, 1448-55 (2003).
- [2] S.-C. Yu, C.-C. Kwok, W.-K. Chan, C.-M. Che, *Adv. Mater.* **15**, 1643-7 (2003).
- [3] M. Kimura, Y. Iwashima, K. Ohta, K. Hanabusa, H. Shirai, *Macromolecules*, **38**, 5055-9 (2005).
- [4] Y. Nishimori, K. Kanaizuka, M. Murata, H. Nishihara, *Chem. Asian J.*, **2**, 367-76 (2007).
- [5] D. Hinderberger, O. Schmelz, M. Rehahn, G. Jeschke, *Angew. Chem. Int. Ed.*, **43**, 4616-21 (2004).
- [6] P. R. Andres, U. S. Schubert, *Adv. Mater.*, **16**, 1043-68 (2004); H. Hofmeier, U. S. Schubert, *Chem. Soc. Rev.*, **33**, 373-99 (2004).
- [7] F. S. Han, M. Higuchi, D. G. Kurth, *Adv. Mater.*, **19**, 3928-31 (2007); F. S. Han, M. Higuchi, D. G. Kurth, *Org. Lett.*, **9**, 559-62 (2007).
- [8] D. G. Kurth, *Ann. N. Y. Acad. Sci.* **960**, 29-38 (2002).
- [9] M. Granmar, A. Cho, *Science*, **308**, 785-6 (2005).
- [10] J. Garín, J. Orduna, S. Uriel, A. J. Moore, M. R. Bryce, S. Wegener, D. S. Yufit, J. A. K. Howard, *Synthesis*, 489-93 (1994).
- [11] M. Higuchi, Y. Otsuka, D. G. Kurth, *Trans. Mater. Res. Soc. Jpn.*, **32**, 425-8 (2007).
- [12] U. S. Schubert, H. Hofmeier, G. R. Newkome, "Modern Terpyridine Chemistry", Wiley-VCH, Weinheim, (2006) pp. 37-44.
- [13] K. Nilson, J. Ahlund, B. Brena, E. Gothelid, J. Schiessling, N. Martensson, C. Puglia, *J. Chem. Phys.*, **127**, 114702 (2007).
- [14] T. Ikeda, M. Asakawa, M. Goto, K. Miyake, T. Ishida, T. Shimizu, *Langmuir*, **20**, 5454-9 (2004).
- [15] D. G. Kurth, M. Higuchi, *Soft Matter*, **2**, 915-27 (2006).
- [16] T. Kitamura, S. Nakaso, N. Mizoshita, Y. Tochigi, T. Shimomura, M. Moriyama, K. Ito, T. Kato, *J. Am. Chem. Soc.* **127**, 14769-75 (2005).

(Received May 12, 2008 ; Accepted December 14, 2007)